Available online at www.sciencedirect.com

ScienceDirect

Energy Procedia 40 (2013) 266 – 275

Energy Procedia

European Geosciences Union General Assembly 2013, EGU

Division Energy, Resources & the Environment, ERE

Deep control on shallow heat in sedimentary basins

Magdalena Scheck-Wenderoth[a]*, Yuriy Petrovich Maystrenko[a,b]

[a]*Helmholtz Centre Potsdam GFZ German Research Centre for Geosciences, Telegrafenberg, D-14473 Potsdam, Germany.*
[b]*Geological Survey of Norway, Postboks 6315 Sluppen, 7491 Trondheim, Norway*

Abstract

We quantify the 3D temperature distribution for a large and structurally complex intra-continental basin based on physical principles and considering a realistic approximation of the sedimentary fill as well as of the underlying crust and lithospheric mantle. Comparing observed temperatures with temperatures predicted by a 3D conductive, steady-state thermal model for the Central European Basin System (CEBS) we find a thick layer of mobilized Zechstein salt causes significant local temperature variations due to its high thermal conductivity compared to less conductive surrounding clastic sediments. This local pattern is superposed by a regional component originating in the deeper lithosphere.

Keywords: heat flow, geothermal energy, thermal model, deep temperatures, sedimentary basin

1. Introduction

Temperature distribution in sedimentary basins controls the fate of petroleum or geothermal heat resources and the mode of deformation of the lithosphere. So far regional temperature estimates for the subsurface largelenly rely on interpolation of local measurements in wells (LIAG, [1]) or thermal models

* Corresponding author. Tel.: +49-331-2881345; fax: +49-331-2881349.
E-mail address: leni@gfz-potsdam.de.

doi:10.1016/j.egypro.2013.08.031

covering only limited segments of basins (Bjorlykke, [2]). Previous estimates of the relative contribution of heat from different depths of the lithosphere are largely based on 1D or 2D calculations and the additional influence of 3D heat transfer remains uncertain (Artemieva, [3]; Jaupart, [4]; Mareschal and Claude, [5]). This is due to a scarcity of regional studies addressing heat transfer in 3 dimensions for realistic data sets (Scheck-Wenderoth and Maystrenko [6]). Also, previous thermal models of north central Europe were either restricted to a segment of the sedimentary part (Bayer et al., [7]; GEUS, [8]; LIAG, [1]; Norden et al., [9]; Noack et al., [10]) or theoretical and based on strongly simplified configurations (Cloetingh et al., [11]; Tesauro et al., [12]). With our model we evaluate how and why subsurface temperature varies over this area and test two hypotheses: (1) that heat in sedimentary basins is dominantly transferred by thermal conduction and (2) that 3D thermal models considering basin configuration can predict subsurface temperature distribution beyond the initial database.

1.1 Geological background and method

The CEBS (Fig. 1) is an area with an exceptionally good coverage of geological and geophysical data as a consequence of hydrocarbon exploration and academic research programs. This has enabled the construction of a lithosphere-scale regional 3D structural model (Fig. 1; Maystrenko et al., [13]; Maystrenko and Scheck-Wenderoth, [14]) which integrates what is probably the world's largest amount of data for a basin system. This model is used to calculate the thermal field and integrates a Precambrian lithosphere in the north-east that adjoins a lithosphere with Caledonian and Variscan consolidation ages below the largest part of the CEBS. More than 10 km of Permian to Cenozoic deposits, including numerous salt structures, rest above an older succession of Pre-Permian deposits. A further complexity lies in the different lithosphere blocks that support the basin system and vary considerably in thickness and composition. Such compositional variations are relevant as they determine the amount of radiogenic heat production and the thermal conductivity of rocks. Variations in deep seismic velocities and densities derived from 3D gravity models point to a silicic upper crust, characterized by high radiogenic heat production, and a less productive lower crust of mafic composition ([14]). The thickness of the crystalline crust, that is thermally more conductive than sediments, increases toward the basin margins where the crust is close to or at the surface. Also, the depth position of the isothermal lithosphere-asthenosphere-boundary (LAB), usually taken to coincide with the 1300 C potential temperature isotherm (McKenzie and Priestly [15]), is relevant for the thermal field as it defines the heat input from the deeper mantle. The LAB in our model rises from more than 200 km depth in Precambrian domains in the NE to about 80 km in the Southern North Sea.

To calculate the thermal field we solve the conductive heat equation

$$c\rho(\partial T/\partial t) = \mathrm{div}(\lambda \,\mathrm{grad} T) + S \tag{1}$$

(with c :heat capacity, ρ: density, T: temperature, λ: thermal conductivity, δT: change in temperature per time interval δt, div: operator giving the spatial variation in temperature, gradT: temperature gradient, t: time, and S: radioactive heat production),with a 3-D finite element method (Bayer et al., 1997) for the steady state (δT/δt = 0).

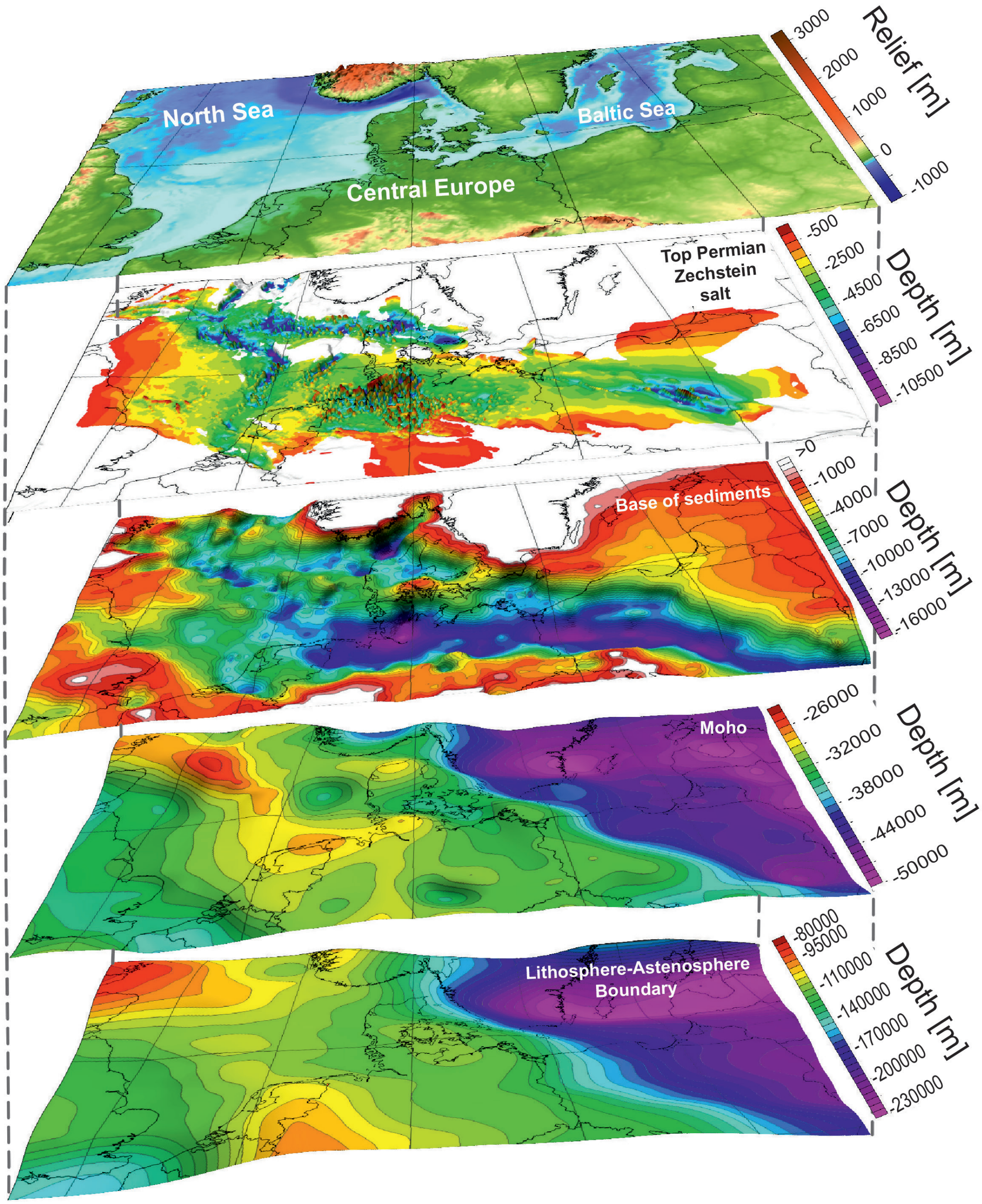

Figure 1. 3D structural model of the CEBS used for thermal calculations with selected surfaces relevant for the thermal field. The model covers about 1000x1800 km with a horizontal resolution of ~4 km and resolves 8 sedimentary units including a layer of mobilized Upper Permian Zechstein salt, 2 layers of the crystalline crust and the lithospheric mantle (after Maystrenko et al., [13]; Maystrenko and Scheck-Wenderoth, [14]).

Thermal properties are assigned according to a dominant lithology for each layer (Table 1) to systematically trace the influences of different layers. The values assigned represent “effective” conductivities required to fit observed temperatures. They do not necessarily correspond to rock thermal conductivities, but may be the result of varying fluid content and porosity in concert with specific matrix thermal conductivities.

For the deeper and therefore hotter layers temperature-corrected constant values for different temperature intervals (Cermak and Rybach, [16]) are considered. The values given correspond to the best-fit model, but sensitivity analyses (Noack et al., [10]) have shown that the contrast between different units is robust. Noteworthy are the high thermal conductivity for the salt as well as for the crystalline crust and the high radiogenic heat production in the upper crystalline crust. The latter varies for the different crustal domains according to consolidation ages with highest values for Variscan granites and for the Variscan upper crust and lowest values for the Precambrian upper crust. The thermal boundary conditions set are a constant temperature of 8°C at the surface, a constant temperature of 1300°C at the LAB that defines the lower boundary of the model, and closed lateral boundaries. Vertically, the model resolves 17 layers and the horizontal resolution of 4 km captures the major salt structures (Maystrenko et al. [13]).

Table 1: Thermal properties and dominant lithologies assigned in the model

Layer of the 3D model	Thermal conductivity k [W/mK]	Heat production S [$\mu W/m^3$]
Cenozoic (clastics)	1.5	0.7
Cretaceous (carbonates and clastics)	1.95	1.0
Jurassic (clastics)	2.1	1.6
Triassic (clastics and carbonates)	2.1	1.6
Zechstein (mainly salt)	3.5	0.3
Zechstein (carbonates, anhydrites and clastics)	1.95	0.8
Rotliegend (clastics)	3	1.5
Permo-Carboniferous volcanics	2.5	2.4
Pre-Permian rocks (clastics)	2.9	1.5
Bohemian granites	3.1	2.9
Variscan upper crystalline crust	2.8	1.3
Felsic Middle-upper cryst. crust of Laurentia	2.8	1.2
Felsic Middle-upper cryst. crust of Avalonia	2.9	1.3
Felsic Middle-upper cryst. crust of Baltica	2.75	0.9
Mafic Lower crust	2.7	0.8
Lithospheric mantle (Peridotite@500-1300°C)	3.95	0.03

2. Results

Main modelling results are illustrated in Fig. 2. Comparing the thickness distribution of the salt (Fig. 2A) with the modelled temperature distribution at 3 km depth (Fig. 2C) and the predicted surface heat flow pattern (Fig. 2G), a clear spatial correlation of local temperature anomalies above salt structures is evident. These variations are related to the more efficient heat transport in the highly conductive salt than in the surrounding low-conductive sediments. Lateral differences in temperature reach up to 40° K at 3 km depth (Fig. 2C) and calculated surface heat flow varies from 50 mW/m2, in areas where salt is absent, to 120 mW/m2 above major salt structures.

This pattern of localized temperature variations is superimposed on a regional pattern displaying colder temperatures at the basin margins opposed to higher temperatures in the basin due to the blanketing effect of the sedimentary fill, which on average is less conductive than the crystalline crust. In particular the uppermost layer of uncompacted Cenozoic clastic sediments (Fig. 2 B) exerts a strongly insulating effect. The basin margins are colder as there the shallow and more conductive crystalline crust (Fig. 1) allows efficient cooling of the upper ~20km. Below the salt layer, the extreme lateral temperature variations fade at more than 8 km depth (Fig. 2D), where the regional pattern of a hotter basin and colder margins prevails. At 30 km depth (Fig. 2E) the area of highest temperature is shifted south and at 60 km depth (Fig. 2F) the temperature distribution shows regionally diffuse lateral variations of up to 400° K. At this depth and below, the influence of the lower boundary condition becomes dominant. Testing different geometries for the LAB (Artemieva, [3]; Jones et al., [17]; Gregersen et al. [18]; Geissler et al. [19]; Plomerova and Babuska, [20]) we find that those consistent with observed temperatures and gravity are in good agreement with LABs derived from seismological observations ([18], [19]). In contrast shallower depths of the LAB as derived by anisotropy studies ([20]) predict hotter temperatures in the sedimentary part than observed. This result confirms the discrepancies concerning LAB depth detected by different methods. Most of the published information on LABs is difficult to compare directly with our 3D model as it relates to different assumptions for the crustal configuration and the reference model.

A comparison of the calculated surface heat flow with published heat flow density maps (Hurter and Schellschmidt, [21]; Majorowicz and Wybraniec, [22]) shows a good correlation with the major trends and the range of heat flow values of the published maps with a closer similarity to maps considering paleoclimatic correction. However, the published heat flow maps do not resolve the short-wavelength variations caused by salt structures but display wider domains of elevated heat flow over areas with abundant salt structures. Comparing the heat flow predicted for the surface (Fig. 2G) with that predicted for the base of sediments (Fig. 2H) and for the Moho (Fig. 2I) shows that about half of the heat reaching the surface is created in the crust where the radiogenic contribution to the heat budget strongly controls the regional thermal field. Predicted heat flow at the Moho (Fig. 2I) ranges between 15 mW/m2 for thick, old lithosphere in the NE, and 50 mW/m2, for the thinnest lithosphere. This spread of 35 mW/m2 is the superposed result of differing LAB depth and laterally variable heat transfer in the crust.

Temperature values are extracted from the model where published observations (Appendix A) are available for comparison (Figure 2 J, K). As these data points (Fig. 2 J and K) relate to wells situated at different depths or stratigraphic intervals and with different distance to salt structures, the range is large for both observed and modelled temperatures. Nevertheless the correlation between observed and calculated values testifies that the model predicts observations reasonably well, that it largely resolves the spatial distribution of thermal properties and thus allows predictions of deep temperatures for areas beyond well control. We find largest misfits to correlate with large fault structures. Also the model is too hot for Precambrian Baltica, in spite of a reduced radiogenic heat production and a deep LAB.

Major uncertainties of the model are related to (1) the model resolution, which does not capture the full structural complexity or lateral changes in lithology, (2) to the assumption of steady state conditions that may be questioned for the Southern North Sea, where rapid Neogene sedimentation occurred and for areas influenced by Quaternary glaciations, and (3) to neglecting fluid transport in the sedimentary layers and along faults.

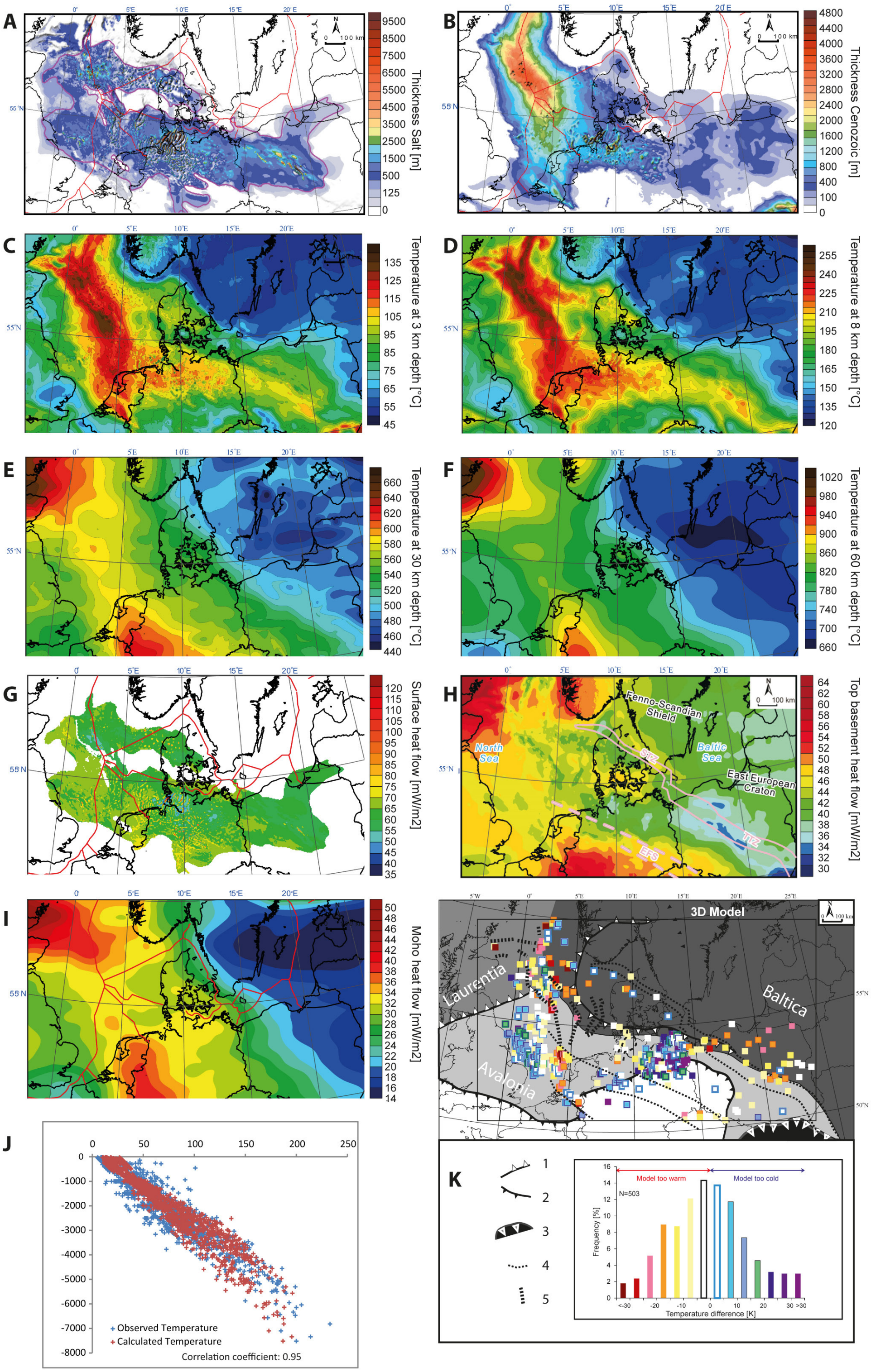

A
Thickness Salt [m]
B
Thickness Cenozoic [m]
C
Temperature at 3 km depth [°C]
D
Temperature at 8 km depth [°C]
E
Temperature at 30 km depth [°C]
F
Temperature at 60 km depth [°C]
G
Surface heat flow [mW/m2]
H
Top basement heat flow [mW/m2]
Fenno-Scandian Shield
North Sea
Baltic Sea
East European Craton
STZ
TTZ
EFS
I
Moho heat flow [mW/m2]
J
Observed Temperature
Calculated Temperature
Correlation coefficient: 0.95
K
3D Model
Laurentia
Baltica
Avalonia
Model too warm
Model too cold
N=503
Frequency [%]
Temperature difference [K]

Figure 2: A: thickness Zechstein salt; B: thickness Cenozoic (A,B after [13]); C,D,E,F: modelled temperature at 3, 8, 30, 60 km depth; G, H,I: modelled heat flow at: surface, base sediments, Moho. White gaps in the surface heat flow map indicate that there surface heat flow corresponds to heat flow at top basement (panel H), which is cropping out. J: observed (blue) versus calculated (red) temperatures against depth for 1689 measured values in 509 wells. K: regional distribution of misfit calculated as the difference between observed and calculated temperatures for those wells where only bottom-hole temperatures were available and as the arithmetic average of the deviation for those wells where we had temperature values for different depths. The misfit is shown against the background map of crustal provinces. Legend key: 1:Caledonian Deformation Front, 2: Variscan Deformation Front (white domain south of the latter corresponds to the Variscan crustal domain); 3: Alpine Deformation Front; 4: large fault zones; 5: large Mesozoic graben structures.

3. Conclusions

Our results support the theory that conductive heat transport is the dominant mechanism of heat transfer in sedimentary basins on a regional scale and we quantify three main factors controlling the deep thermal field, the effects of which are superposed: (1) the internal configuration and related contrasts in thermal properties of the sedimentary layers control the pattern of local (km-scale) temperature variations; (2) the heterogeneous physical properties in the underlying crystalline crust and (3) the depth to the thermal lithosphere-asthenosphere boundary control the regional (100km-scale) pattern of temperature variation. For the upper few km this results in significantly higher temperatures in the basin compared to colder basin margins and in pronounced local thermal anomalies, where large contrasts in thermal conductivity exist near salt structures.The hottest parts of north central Europe are the Southern North Sea, the Netherlands and NW Germany as there the three effects are superposed in a specific way: (1) the low-conductive sedimentary cover is thickest, (2) heat input is focused by numerous large salt structures and (3) the isothermal LAB is shallowest.

Novel is that our model explains observed large lateral variation of temperatures at exploration depths of 3-5 km and quantitatively predicts the thermal regime for areas not covered by measurements. Moreover the model provides boundary conditions for local reservoir models but also for lithosphere-scale models of stress and strain.

Acknowledgements

We thank U. Bayer, M. Cacace, J. Sippel and B. Lewerenz for thermal input. The work was partly supported by DFG SPP1135 and by the German Federal Ministry of Education and Research in the programme “Spitzenforschung in den neuen Ländern” (BMBF Grant 03G0671A/B/C).

References

[[1] LIAG: Subsurface temperature of Germany in different depth. 2012 <http://www.liag-hannover.de/en/online-services-downloads/downloads/maps.html> .

[2] Bjorlykke K. Heat Transport in Sedimentary Basins. Petroleum Geoscience, Springer Berlin Heidelberg, 2010, p. 253-257.

[3] Artemieva I M.. Global 1° × 1° thermal model TC1 for the continental lithosphere: Implications for lithosphere secular evolution: Tectonophysics 2006, **416**, 1-4: 245-277.

[4] Jaupart C, Mareschal J-C. Heat flow and thermal structure of the lithosphere. Treatise on Geophysics 2007. **6**: 217-251.

[5] Mareschal J-C, Claude, J. Energy Budget of the Earth, in Gupta, H. K., ed., Encyclopedia of Earth Sciences Series: 3300 AA Dordrecht, The Netherlands, Springer 2011, p. 285-291.

[6] Scheck-Wenderoth M., Maystrenko Y. How warm are passive continental margins? A 3D lithosphere-scale study from the Norwegian margin. Geology 2008, **36**,. 5: 419-422.

[7] Bayer U, Scheck M, Koehler M. Modeling of the 3D thermal field in the northeast German basin: Geologische Rundschau 1997. **86**, 2: 241-251.

[8] GEUS. Well data summary sheets, Volume 2007, Geological Survey of Denmark and Greenland.

[9] Norden B, Förster A, Balling N. Heat flow and lithospheric thermal regime in the Northeast German Basin. Tectonophysics 2008. **460**: 215-229.

[10] Noack V., Scheck-Wenderoth M. Sensitivity of 3D thermal models to the choice of boundary conditions and thermal properties: a case study for the area of Brandenburg (NE German Basin). Environmental Earth Sciences 2012. **6**, 76: 1695-1711.

[11] Cloetingh S, van Wees J D, Ziegler P A, Lenkey L, Beekman F, Tesauro M, Förster A, Norden B, Kaban M, Hardebol N, Bonté D, Genter A, Guillou-Frottier L, Ter Voorde M, Sokoutis D, Willingshofer E, Cornu T, Worum G. Lithosphere tectonics and thermo-mechanical properties: An integrated modelling approach for Enhanced Geothermal Systems exploration in Europe: Earth-Science Reviews2010. **102**, 3-: 159-206.

[12] Tesauro M, Kaban M K, Cloetingh S. A new thermal and rheological model of the European lithosphere: Tectonophysics 2009. **476**: 478-495.

[13] Maystrenko Y P, Bayer U, Scheck-Wenderoth M. Salt as a 3D element in structural modeling - Example from the Central European Basin System. Tectonophysics 2012b online first.

[14] Maystrenko YP, Scheck-Wenderoth M. 3D lithosphere-scale density model of the Central European Basin System and adjacent areas, Tectonophysics 2013, http://dx.doi.org/10.1016/j.tecto.2013.04.023

[15] McKenzie D, Priestley K. Thermal structure of oceanic and continental lithosphere: Earth and Planetary Science Letters 2005. **233**, 3-4: 337-349.

[16] Cermak V, Rybach L. Thermal properties: Thermal conductivity and specific heat of minerals and rocks. Landolt-Börnstein, New Series, Geophysics and space research. G. Angenheister. Berlin, Springer. 1a, 1982: 305–343.

[17] Jones A G, Plomerova J, Korja T, Sodoudi F, Spakman W. Europe from the bottom up: A statistical examination of the central and northern European lithosphere-asthenosphere boundary from comparing seismological and electromagnetic observations: Lithos 2010. **120**, (1-2), p. 14-29.

[18] Gregersen S, Voss P, Nielsen L V, Achauer U, Busche H, Rabbel W, Shomali Z H. Uniqueness of modeling results from teleseismic P-Wave tomography in Project Tor: Tectonophysics 2010. **481**, 1-4: 99-107.

[19] Geissler W H, Sodoudi F. Kind R. Thickness of the central and eastern European lithosphere as seen by S receiver functions: Geophysical Journal International 2010. **181**, 2: 604-634.

[20] Plomerová J, Babuska V. Long memory of mantle lithosphere fabric -- European LAB constrained from seismic anisotropy: Lithos 2010. **120**,. 1-2: 131-143.

[21] Hurter S, and Schellschmidt R, Heat Flow Density. In Hurter, S. and Haenel, R. (eds), Atlas of Geothermal Resources in Europe: Luxemburg Office for Official Publications of the European Communities. 2002.

[22] Majorowicz J, Wybraniec S, New terrestrial heat flow map of Europe after regional paleoclimatic correction application: International Journal of Earth Sciences. 2010

Appendix A. Sources of database for observed temperatures

Andrews-Speed, C.P., Ron Oxburgh, E., Cooper, B.A., 1984. Temperatures and depth-dependent heat flow in western North Sea. AAPG Bulletin, 68 (11), 1764-1781.

Argent, J. D., Stewart, S. A., Green, P. F., & Underhill, J. R., 2002. Heterogeneous exhumation in the Inner Moray Firth, UK North Sea: constraints from new AFTA and seismic data. Journal of the Geological Society, London, Vol. 159, pp. 715–729.

Bujakowski, W., Barbacki, A., Czerwinska, B., Pajak, L., Pussak, M., Stefaniuk, M., Trzesniowski, Z., 2010. Integrated seismic and magnetotelluric exploration of the Skierniewice, Poland, geothermal test site. Geothermics 39, 78–93.

Förster, A., 2001. Analysis of temperature data in the Northeast German Basin: continuous logs versus bottom-hole temperatures. Petroleum Geoscience, 7, 241–254.

Geothermisches Informationssystem für Deutschland (Geotis), 2011. http://www.geotis.de/, (March 2011).

Geozentrum Hannover (LBEG), 2011. Geothermie - geht das bei mir? http://www.lbeg.niedersachsen.de/portal/live.php?navigation_id=27033&article_id=91279&_psmand=4 (March 2011).

Gladysz, M., Sokolowska, J. and Sokolowski, J., 1993. Geothermal projects in Poland. GHC Quartelny Bulletin 23 (6), 20–25.

Japsen, P., Green, P. F., Nielsen, L. H., Rasmussen, E. S. & Bidstrup, T. 2007. Mesozoic–Cenozoic exhumation in the eastern North Sea Basin: a multi-disciplinary study based on palaeo-thermal, palaeoburial, stratigraphic and seismic data. Basin Research, 19, 451–490.

Eriksson, K. G., Ahlbom, K., Landstrom, O., Larson, S. A., Lind, G. and Malmqvist, D., 1979. Investigation for Geothermal Energy in Sweden. Pageoph, Vol. 117, 196-204.

Kuehn, M. and Guenther, A., 2007. Stratabound Rayleigh convection observed in a 4D hydrothermal reactive transport model based on the regional geological evolution of Allermoehe (Germany). Geofluids, 7(3), 301–312.

Kus, J., Cramer, B., and Kockel, F., 2005. Effects of a Cretaceous structural inversion and a postulated high heat flow event on petroleum system of the western Lower Saxony Basin and the charge history of the Apeldorn gas field. Netherlands Journal of Geosciences - Geologie en Mijnbouw, 84, 3–24.

Leibniz Institute for Applied Geophysics (LIAG), 2011. Online-Dienste & Downloads. http://www.liag-hannover.de/de/online-dienste-downloads/downloads.html (March 2011).

Luijendijk, E., ter Voorde, M., van Balen, R., Verweij, H. and Simmelink, E., 2011. Thermal state of the RoerValley Graben, part of the European Cenozoic Rift System. Basin Research 23, 65–82.

Majorowicz, J., 1979. Mantle Heat Flow and Geotherms for Major Tectonic Units in Central Europe. Pageoph, Vol. 117, 109-123.

Norwegian Petroleum Directorate (NPD), 2007. The NPD's fact pages; well data summary sheets: http://www.npd.no/engelsk/cwi/pbl/en/wdss_index.htm. (March 2011)

Okiongbo, K.S., 2011. Bulk Volume Reduction of the Kimmeridge Clay Formation, North Sea (UK) Due to Compaction, Petroleum Generation and Expulsion. Research Journal of Applied Sciences, Engineering and Technology 3(2), 132-139.

Pester, S., Agemar, T., Alten, J.-A., Kuder, J., Kuehne, K., Maul, A.-A., and Schulz, R., 2010. GeotIS - the Geothermal Information System for Germany. Proceedings World Geothermal Congress, pp. 25–29.

Petmecky, S., Meier, L., Reiser, H., Littke, R., 1999. High thermal maturity in the Lower Saxony Basin: intrusion or deep burial? Tectonophysics 304, 317–344.

Rodon, S. and Littke, R., 2005. Thermal maturity in the Central European Basin system (Schleswig-Holstein area): results of 1D basin modelling and new maturity maps. International Journal of Earth Sciences, 94(5), 815–833.

Schoener, R., 2006. Comparison of Rotliegend sandstone diagenesis from the northern and southern margin of the North German Basin, and implications for the importance of organic maturation and migration. PhD thesis Univ. Jena, 160 pp.

The Global Heat Flow Database of the International Heat Flow Commission, 2011 http://www.heatflow.und.edu/data.html, (March 2011).

Van Balen, R.T., Verweij, J.M., Van Wees, J.D., Simmelink, H., Van Bergen, F., Pagnier, H., 2002. Deep subsurface temperatures in the Roer Valley Graben and the Peelblock, the Netherlands – new results. Netherlands Journal of Geosciences (Geologie en Mijnbouw), 81, 19–26.

Van Balen, R.T., van Bergen, F., de Leeuw, C., Pagnier, H., Simmelink, H., van Wees J.D. & Verweij, J.M.,2000. Modelling the hydrocarbon generation and migration in the West Netherlands Basin, the Netherlands. Geologie en Mijnbouw / Netherlands Journal of Geosciences 79 (1), 29-44.

Vandenberghe, N., Fock, W., 1989. Temperature data in the subsurface of Belgium. Tectonophysics, 164, 237-250.

Verweij, J.M., 2003. Fluid flow systems analysis on geological timescales in onshore and offshore Netherlands, with special reference to the Broad Fourteens Basin. Thesis, Vrije Universiteit (Amsterdam): 278 pp.

Verweij, J.M., Souto Carneiro Echternach, M., Witmans, N., 2010. Central Offshore Platform - Area NCP2E Burial history, temperature, source rock maturity and hydrocarbon generation. TNO report (TNO-034-UT-2010-01298 / A), 70 pp.

Yu, Z., Thomsen R. O. and Lerche, I., 1995. Crystalline basement focusing of heat versus fluid flow/compaction effects: a case study of the 1-1 well in the Danish North Sea. Petroleum Geoscience, Vol. 1, 1995, pp.31-35.

Wohlenberg, J., 1979. The subsurface temperature field of the Federal Republic of Germany. Schweizerbart, Hannover.

Appendix B. Additional Temperature- maps for depths of

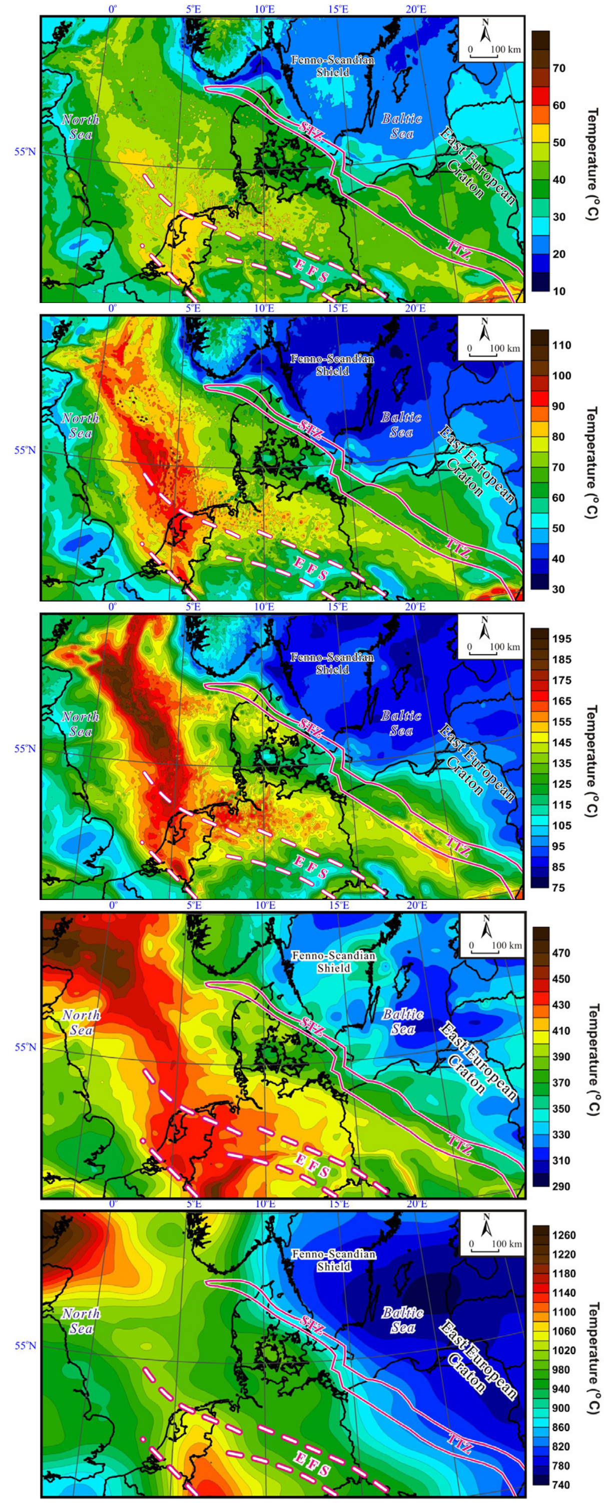

1km,

2 km,

5km,

20 km,

80 km